System-Level Performance of Downlink Non-orthogonal Multiple Access (NOMA) Under Various Environments

Yuya Saito, Anass Benjebbour, Yoshihisa Kishiyama, and Takehiro Nakamura
5G Radio Access Network Research Group, 5G Laboratory, NTT DOCOMO, INC.
Email: yuuya.saitou.fa@nttdocomo.com

***Abstract*—Non-orthogonal multiple access (NOMA) is a promising multiple access scheme for further improving the spectrum efficiency compared to that for orthogonal multiple access (OMA) in the 5th Generation (5G) mobile communication systems. All of the existing evaluations for NOMA focus on the macrocell deployment since NOMA fully utilizes the power domain and the difference in channel gains, e.g., path loss, between users, which is typically sufficiently large in macrocells. Currently, small cells are becoming important and being studied for future Long-Term Evolution (LTE) enhancements in order to improve further the system performance. Thus, it is of great interest to study the performance of NOMA for small cell deployment under various environments. This paper investigates the system level performance of NOMA in small cells considering practical assumptions such as the single user multiple-input multiple-output (SU-MIMO) technique, adaptive modulation and coding (AMC), feedback channel quality indicator (CQI). Some of the key NOMA specific functionalities, including multi-user paring and transmit power allocation are also taken into account in the evaluation. Based on computer simulations, we show that for both macrocell and small cell deployments, NOMA can still provide a larger throughput performance gain compared to that for OMA.**

Keywords—Non-orthogonal multiple access, NOMA, successive interference canceller, MIMO, rank adaptation

I. INTRODUCTION

Nowadays, discussions on the Long-Term Evolution (LTE) and LTE-Advanced toward 2020 and beyond are becoming increasingly important since rapid growth in the volume of mobile data such as that from smartphones and new mobile devices, which support a wide range of applications and services, demands a future concept for radio access technologies and new technical solutions that can respond to future challenges and requirements, including higher capacity and higher quality of user experience (QoE) levels. To this end the 3rd Generation Partnership Project (3GPP) started discussions on further steps in the evolution of LTE toward the future, i.e., Release 12 and onwards [1]. Furthermore, some initial discussions on the 5th generation (5G) mobile communication systems are taking place in the radio communication sector of the international telecommunications union radio (ITU-R) and are being led by multiple projects and companies [2, 3].

The most important requirement for the 5G systems is the provision of higher system capacity. Many recent forecasts project that the volume of mobile data traffic will grow beyond 24 fold between 2010 and 2015 [4], and thus beyond 1000 fold in 10 years (2010-2020) assuming that the same rate of growth is maintained. Therefore, the capacity of future systems must be increased immensely to deal with the growth in traffic volume. In addition, providing a better user experience by improving the achievable data rates, and fairness in the user throughput and latency are important requirements. Another important requirement is the efficient support for a variety of traffic types, including a reduction in the impact of the ever-increasing volume of signaling traffic both on the network and handheld device sides, the support of lower latency for the currently proliferating cloud services, and the handling of simultaneous connections from a large number of small data packets for machine-to-machine (M2M) traffic. Over the past few years, we presented our 5G concept and candidate technologies in order to satisfy these requirements [5]. Specifically, our concept involves a combination of efficient utilization and integration of higher and wider frequency bands for capacity and data rate enhancement along with lower frequency bands for both macrocells and small cells.

To improve further the spectrum efficiency in 5G, we proposed a downlink Non-orthogonal multiple access (NOMA) scheme as a candidate multiple access scheme in a lower frequency band [6]. Specifically, multiple users are multiplexed in the power domain on the transmitter side and multi-user signal separation on the receiver side is performed based on successive interference cancellation (SIC). There has already been some research on the performance gain of NOMA compared to orthogonal multiple access (OMA) based on OFDMA in the cellular downlink [7-11]. Most studies on NOMA focus on NOMA with single-input multiple-output (SIMO) [7,10], but some reports discuss the combination of NOMA with multiple-input multiple-output (MIMO) technology, including single user MIMO (SU-MIMO) and multi-user MIMO [8, 9, 11]. In addition, some key NOMA technologies related to multi-user scheduling and multi-user power allocation, which requires a new design compared to the current LTE radio interface, were investigated [9]. In order to support NOMA in 5G, further investigations are required that include different deployment scenarios considering some practical simulation assumptions. For example, further discussions on small cell enhancements are currently ongoing in order to improve the system performance of (dense) small cell deployments in [2] and [12]. Therefore, small cell deployment should also be considered and discussed in NOMA. However, all of the existing evaluations mentioned above are based on macrocells that have a relatively longer

inter-site distance (ISD) and higher base station (BS) transmit power than those for a small cell.

This paper investigates the performance gain of NOMA in a small cell deployment. Downlink performance of NOMA is evaluated and compared to OMA based on system-level simulations with practical assumptions such as the feedback channel quality indicator (CQI), adaptive modulation and coding (AMC), and the single-user (SU) MIMO technique according to the LTE/LTE-A specifications [13]. Simulation results show that, similar to a macrocell, NOMA in a small cell with various environments can provide a large performance gain compared to that for OMA.

The rest of the paper is organized as follows. Section II gives a detailed description of the system model for NOMA with SIC in SU-MIMO in the cellular downlink. In Section III, the major simulation assumptions and parameters for the system-level evaluation are shown. Then, the results of the performance of NOMA in small cells with various environments compared to that for OMA are provided and discussed in Section IV. Finally, we present our conclusions in Section V.

II. System Model

This section describes the system model of NOMA with SU-MIMO. The basic MIMO features, techniques available in the LTE downlink, and some of the key features of NOMA with SIC are discussed in detail below.

A. NOMA with Open loop MIMO

LTE Release 8 supports several transmission modes that are designed to take full advantage of the channel conditions, eNodeB (eNB) antenna configurations, and differences in the user equipment (UE) capabilities and mobility. In this paper, open loop (OL) MIMO with SU-MIMO is a baseline operation. This is because the OL operation is at the core of LTE MIMO techniques and is preferable when the UE is moving too fast to provide a detailed report on the channel conditions in time for the eNB. In OL operation, there are two types of transmission schemes supported in LTE Release 8 [13]. For example, Space-frequency block coding (SFBC) which is used to encode the same data differently and boost signal and interference to noise ratio (SINR) of the recombined data streams in order to obtain the transmit diversity. In addition, spatial multiplexing can be adopted to send completely different data through each transmit antenna precoder to increase the system capacity [11]. Note that each set of data sent through the transmit antenna precoders in a spatial multiplexing operation is called a layer in LTE.

B. Adaptive Modulation and Coding and Rank Adaptation

The selection of each transmission mode depends on whether the UE is able to provide detailed and timely information regarding its channel conditions. Specifically, the eNB receives the following information from the UE: a rank indicator (RI), which is the number of layers that can be supported under the current channel conditions and modulation and coding scheme (MCS), and a channel quality indicator (CQI), which reports information of the channel conditions under the current transmission mode, roughly corresponding to SINR. In this paper, rank adaptation, which is supported in LTE Release 8, is also considered. Thus, the number of layers is adaptively controlled according to the channel conditions. In addition, both OMA and NOMA adopt AMC to provide the flexibility to match the MCS to the average channel conditions for each user.

C. Signal Model of NOMA with SIC in SU-MIMO

In this paper, we assume that the total transmit bandwidth, BW, is divided into S subbands, where the bandwidth of each subband is B ($BW = S \times B$). In each subband, the eNB performs downlink transmission to multiple users simultaneously at different transmission power levels for different users. Throughout this paper, the number of subbands, S, and the maximum number of multiplexing users, N_{max}, is equal to one and two, respectively. We also assume that the number of transmitter antennas at the UE is 2 ($N_t = 2$), while the number of receiver antenna at the UE is 2 ($N_r = 2$) where up to 2 layers ($m = 1, 2$) are supported. Without loss of generality, received signal vector $y(l,m)$ at UE_l ($l = 1, 2$) is represented by

$$y(l,m) = h(l) \cdot \left(w(1) \cdot \sqrt{P\alpha_1} \cdot x(1,m) + w(2) \cdot \sqrt{P\alpha_2} \cdot x(2,m)\right) + n(l,m), \quad (1)$$

for

$$h(l) = \begin{bmatrix} h_{11}(l) & h_{12}(l) \\ h_{21}(l) & h_{22}(l) \end{bmatrix}, w(l) = \begin{bmatrix} w_{11}(l) & w_{12}(l) \\ w_{21}(l) & w_{22}(l) \end{bmatrix},$$
$$x(l,m) = \begin{bmatrix} x(l,1) \\ x(l,2) \end{bmatrix}, n(l,m) = \begin{bmatrix} n(l,1) \\ n(l,2) \end{bmatrix}, \quad (2)$$

where $h(l)$ and $w(l)$ denote the $N_t \times N_r$-dimensional channel response matrix and precoding matrix for UE_l, respectively. Terms $x(l,m)$ and $n(l,m)$ denote the N_r-dimensional transmission signal and noise plus inter-cell interference vector for each layer at UE_l, respectively. The total transmission power of the eNB is equal to P. Thus, the sum power constraint is $\alpha_1 + \alpha_2 = 1$. At the receiver, the minimum-mean-squared error (MMSE) is applied to $y(l,m)$ as indicated below.

$$\tilde{y}(l,m) = G(l) \cdot y(l,m) = G(l) \cdot h(l) \cdot \left(w(1) \cdot \sqrt{P\alpha_1} \cdot x(1,m) + w(2) \cdot \sqrt{P\alpha_2} \cdot x(2,m)\right) + G(l) \cdot n(l,m) \quad (3)$$

$$G(l) = \begin{bmatrix} g_{11}(l) & g_{12}(l) \\ g_{21}(l) & g_{22}(l) \end{bmatrix} = Z^H(l)\left(Z(l) \cdot Z^H(l) + \sigma^2 \cdot E\right)^{-1} \quad (4)$$

where $Z(l)$ is an equivalent channel matrix of UE_l defined as $Z(l) = h(l) \cdot w(l)$. Terms $G(l)$, σ^2, and E denote the MMSE weight and noise power of UE_l and identity matrix, respectively. Assuming that the receiver of UE_1 is able to perfectly remove the inter-user interference from UE_2 by applying SIC, the equivalent transmission signal of UE_1 from (3) and (4) is given by

$$\tilde{y}(1,m) = (V(1) \cdot \sqrt{P\alpha_1} \cdot x(1,m)) + N_e(1,m) \quad (5)$$

for

$$V(l) = G(l) \cdot Z(l) = \begin{bmatrix} v_{11}(l) & v_{12}(l) \\ v_{21}(l) & v_{22}(l) \end{bmatrix},$$
$$N_e(l,m) = G(l) \cdot n(l,m) = \begin{bmatrix} n_e(l,1) \\ n_e(l,2) \end{bmatrix}, \quad (6)$$

where $V(l)$ is defined as the equivalent channel matrix including the MMSE weight of UE_l. Term $N_e(l,m)$ denotes the equivalent noise at the receiver of UE_l on layer m. Based on (5) and (6), the equivalent SINR, $SINR(1,m)$, of the desired signal on each layer is represented as

$$SINR(1,m) = \frac{|v_{mm(1)}|^2 \alpha_1 P}{|v_{mk,m\neq k(1)}|^2 \alpha_1 P + |n_e(1,m)|^2} \quad (7)$$

where m, k = 1, 2. Note that (7) is equal to the SINR for an OMA user and is utilized for the rank selection. In this paper, the NOMA users with SIC are determined based on the user throughput. To achieve this, at the eNB, the expected throughput of each candidate user set is computed using feedback CQI, which is also obtained using (7). Then, a NOMA user with higher expected user throughput applies SIC to remove the interference from other users, while UE_2 directly decodes its own signal. Assuming that the signal of UE_1 is treated as interference, the equivalent transmission signal of UE_2 is then given by

$$\tilde{y}(2,m) = \left(V(2) \cdot \sqrt{P\alpha_2} \cdot x(2,m) + U \cdot \sqrt{P\alpha_1} \cdot x(1,m)\right) + N_e(2,m) \quad (8)$$

for

$$U = \begin{bmatrix} u_{11} & u_{12} \\ u_{21} & u_{22} \end{bmatrix} = G(2) \cdot h(2) \cdot w(1). \quad (9)$$

Based on (8) and (9), the equivalent SINR of UE_2 on each layer, $(2,m)$, is represented as

$$SINR(2,m) = \frac{|v_{mm(2)}|^2 \alpha_2 P}{|v_{mk,m\neq k(2)}|^2 \alpha_2 P + \left(|u_{mm}|^2 + |u_{mk,m\neq k}|^2\right)\alpha_1 P + |n_e(2,m)|^2}. \quad (10)$$

D. Transmission Power Allocation

In NOMA, transmission power allocation (TPA) to one user affects the achievable throughput of not only that user but also the throughput of other users. Exhaustive full search of user pairs and transmit power allocations yields the best TPA performance in NOMA. However, this approach incurs a high level of computational complexity since all possible power allocation combinations and user pairs are considered to find best candidate users and power allocation. To reduce the computational complexity, some of the novel power allocation schemes have been proposed. For example, pre-defined user grouping and per-group fixed power allocation has been demonstrated in [9]. In the paper, the full search power allocation scheme in [11] with 10 power sets is utilized.

E. Scheduling Algorithm

Fig. 1 shows a system flow chart, including the selection of the user set and TPA of NOMA for the performance evaluation. Once the OMA based CQI reported from the UEs is available, the eNB schedules the resource allocation of the UE by considering the approximated SINR described in [11]. In this paper, the proportional fair (PF) scheduling algorithm described in [7] is utilized. Specifically, candidate user sets including the TPA and MCS are determined based on the following criteria

$$\max_{U,P} \sum_{l\in U} \left(\frac{\tau(l|U,P)}{\bar{T}^{\alpha}(l)}\right),$$

where U denotes the candidate user set. Terms $\bar{T}(l)$ and $\tau(l|U,P)$ denote the average throughput and instantaneous throughput of UE_l, respectively. P denotes the allocated power sets and α is the weighing factor. When α is equal to 0, maximum sum-rate scheduling is achieved, while proportional fair scheduling is performed when α is equal to 1. As α is further increased, there are more opportunities to be scheduled for the cell-edge user. In this paper, the performance gain of NOMA using a wideband MCS is assumed for the performance measurement.

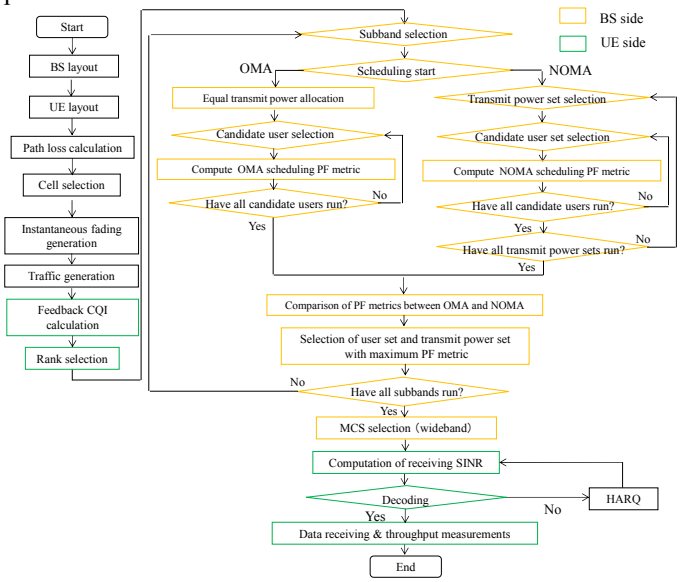

Fig. 1. System flow chart of NOMA with SU-MIMO.

III. Simulation Assumptions and Parameters

To investigate the system performance of NOMA considering practical assumptions such as the CQI feedback, AMC, and MIMO, we conduct a multi-cell system-level simulation is conducted. The major simulation parameters based on the existing LTE/LTE-Advanced specifications [13] are utilized as summarized in Table I. We mainly evaluate a small cell environment and compare it to a macrocell environment. In order to emulate the small cell environment, our simulation assumptions follow the simulation guidelines of the METIS project described in [2]. For comparison, the major simulation parameters for the macrocell deployment described in [7] are also utilized in the simulation. We employed a 19-hexagonal small cell model with 3 sectors per cell. The cell radius of the small cells is set to 115 m. The locations of the UEs are assigned randomly with a uniform distribution. In the propagation model, we take into account distance-dependent path loss, lognormal shadowing with standard deviation, and instantaneous multipath fading from ITU urban Micro (UMi) channel model described in [13] with different outdoor UE ratios. The maximum Doppler frequency, fd, is set to 5.55 Hz, which corresponds to 3 km/h at the carrier frequency of 2 GHz. The system bandwidth is set to 20 MHz and the transmission power of the small cells is 44 dBm. The antenna gain in the small cell and at the UE is 17 dBi and 0 dBi, respectively. Two-antenna transmission and two-antenna reception with OL MIMO (Transmission mode 3 in Rel. 8 LTE) are assumed. The 20 MCS sets are used for AMC in the performance evaluation [10]. A full buffer traffic model is employed. The feedback delay is modeled such that the CQI is not available for scheduling until 6 subframes after the periodic report with a 10 ms interval. In addition, the rank report interval is set to 100 ms. Note that more than two users can be multiplexed in NOMA. For example, the performance gain of NOMA when N_{max} is equal to 3 was investigated in [10] and about 1% improvement of the NOMA gain for cell throughput was obtained compared to that when N_{max} is equal

to 2. However, more multiplexing users gives more complex processing of SIC at receiver side. Thus, N_{max} is set to 2 in the evaluation.

Concerning the radiation pattern of small cell, vertical plane is represented as [14]

$$A_{E,V}(\theta) = -min\left[12\left(\frac{\theta - 90^\circ}{\theta_{3dB}}\right), SLA_V\right], \theta_{3dB} = 65^\circ, SLA_V = 30,$$

whereas horizontal plane is calculated as

$$A_{E,H}(\varphi) = -min\left[12\left(\frac{\varphi}{\varphi_{3dB}}\right), A_m\right], \varphi_{3dB} = 65^\circ, A_m = 30.$$

The combination of both planes is

$$A_E(\theta, \varphi) = -min\{-[A_{E,V}(\theta) + A_{E,H}(\varphi)], A_m\}.$$

The main difference of the radiation pattern between macrocell and small cell is that the vertical gain of small cell is larger than that of macrocell for almost all θ, while the horizontal gain is the same.

TABLE I. SIMULATION PARAMETERS

Cell layout	Hexagonal grid, 19 cell sites, 3 cells per site
Inter-site distance (ISD)	200 m, 500 m
Minimum distance between UE and cell site	10 m for ISD = 200 m, 35 m for ISD = 500 m
Channel model, distance dependent path loss, and shadowing standard deviation	ITU UMi [13] for ISD = 200 m SCM [7] for ISD = 500 m
Total transmission power	44 dBm (25 W) for ISD = 200 m 49 dBm (80 W) for ISD = 500 m
Transmitter antenna gain plus cable loss	17 dBi for ISD = 200 m, 14 dBi for ISD = 500 m
UE antenna gain	0 dBi
UE noise figure	9 dB
Thermal noise density	-174 dBm /Hz
BS and UE antenna configuration	BS: Cro (0.5λ), UE: Cro (0.5λ)
BS antenna height	10 m for ISD = 200 m, 32 m for ISD = 500 m
UE antenna height	1.5 m
Carrier frequency	2 GHz
System bandwidth	20 MHz
Number of sub-carriers	1200
RB bandwidth	180 kHz
Sub-frame length (TTI length)	1.0 ms
Number of subbands	1
Number of UEs per cell	2, 6, 10 for ISD = 200 m, 2, 6, 10, 30 for ISD = 500 m
Outdoor UE ratio	0, 25, 50, 100%
Control delay (scheduling, AMC)	6 ms
HARQ	Chase combining
Round trip delay (HARQ)	8 ms
Outer-loop link adaptation (OLLA)	Off
Granularity of CQI feedback	10 TTIs
Granularity of rank adaptation	100 TTIs
CQI quantization	No
Channel estimation / CQI measurement	Ideal
CQI feedback error	NA
UE receiver assumption	MMSE
Feedback mode	Open Loop
Overhead	0.66

IV. SIMULATION RESULTS AND ANALYSIS

In order to investigate the performance gain of NOMA, the cell throughput and cell-edge user throughput are evaluated based on the following definitions. The cell throughput is defined as the cell throughput for one sector in a small cell (or macrocell), while the cell-edge user throughput is defined as the 5% value of the cumulative distribution function (CDF) of the user throughput. First of all, the user throughput performance for OMA and NOMA with different number of UEs per sector for the macrocell and small cell deployments is evaluated. We assume that all users are assumed located outdoors. The performance, including the cell throughput, cell-edge user throughput, and NOMA gain is summarized in Table II. For comparison purposes, the performance of OMA and NOMA in the macrocell is computed based on 30 UEs per sector where the user density is almost the same as that for 6 UEs per sector in the small cell. The results show that NOMA in the macrocell achieves a cell throughput gain of approximately 31% (cell-edge user throughput gain of 33%), while NOMA in the small cell achieves a cell throughput gain of approximately 35% (cell-edge user throughput gain of 23%). Note that effect of the imperfect cancellation due to the SIC is an important issue and is difficult to directly taken into account in the system-level evaluation. In [9], a worst-case model in order to emulate error propagation of the SIC receiver was demonstrated. This simple model provides a good estimation of the impact of error propagation for NOMA performance. As the evaluation result, the error propagation has marginal impact on NOMA performance. Fig. 2 shows the comparison of user ranking ratio between macrocell and small cell for OMA and NOMA. For comparison, all combination of user rank for NOMA is also included in the figure. As seen, NOMA ratio for macrocell and small cell is about 84% and 65%, respectively. Therefore, we find that NOMA in a small cell can provide a higher performance gain compared to that for OMA. It is also seen that NOMA gain for cell throughput in small cell is larger than that in macrocells. This is because the user ranking ratio with both paired users are of rank 2 is larger for small cells than macrocells. Fig. 3 shows the CDF of the geometry for OMA in the macrocell and small cell, which is defined as the SINR including the path loss and shadowing in the simulation. The figure shows that almost the same performance trend occurs although the geometry for small cells is better than that for the macrocell at a high user

TABLE II. PERFORMANCE COMPARISON BETWEEN MACROCELL AND SMALL CELL

ISD (m)	Number of UEs per Sector	Cell (Mbps)			Cell-Edge (Mbps)		
		OMA	NOMA	Gain (%)	OMA	NOMA	Gain (%)
200	6	48.1357	64.8829	34.79	0.962962	1.187087	23.27
500	30	39.0437	51.2937	31.38	0.28688	0.381453	32.97

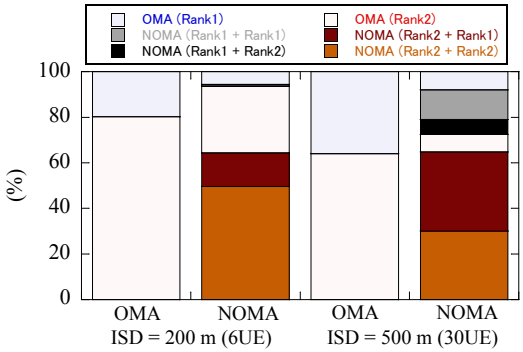

Fig. 2. Comparison of user ranking ratio between macrocell and small cell for OMA and NOMA.

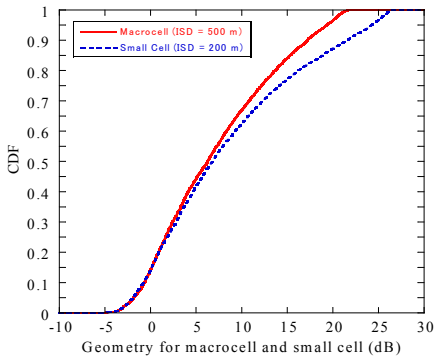

Fig. 3. CDF of geometry for OMA in macrocell and small cell.

throughput. This indicates that the difference in channel gain between paired UEs in the evaluation is sufficiently large to obtain good NOMA performance gain even for small cells where the distance between UEs is relatively shorter compared to that in the case of macrocells.

To investigate further the performance of NOMA, different outdoor UE ratios are considered. Fig. 4 shows the cell throughput and cell-edge user throughput for both OMA and NOMA, and the NOMA gain with different numbers of UEs per sector and different outdoor UE ratios in a small cell. The figure shows that NOMA exhibits higher cell throughput and cell-edge user throughput performance levels compared to those for OMA. The results show that NOMA is useful even when 100% of the UEs are indoors and the small cell is outdoors. We also see that the performance gain in the cell throughput and cell-edge user throughput for both OMA and NOMA is increased when the number of UEs is increased. This is because the multiuser diversity gain is obtained.

Finally, throughput performance of OMA and NOMA with different value of α is investigated. Fig. 5 shows how s affects the throughput performance, including cell and cell edge user throughput for OMA and NOMA with 6 UEs per sector in the small cell. As seen, NOMA gain is improved when h becomes large. For example, the cell throughput gain of NOMA with respect to OMA is about 45% for a given cell-edge user throughput at 0.96 Mbps, while about 66% of NOMA gain is achieved at 1.61 Mbps of cell-edge user throughput. Thus, NOMA can provide better performance even for different value of α for the PF scheduling metric.

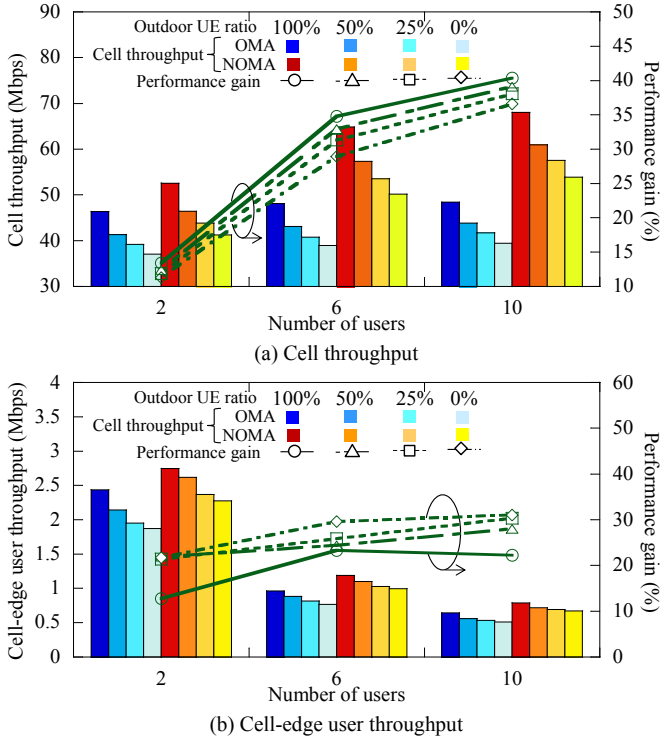

(a) Cell throughput

(b) Cell-edge user throughput

Fig. 4. Throughput performance of OMA and NOMA with different outdoor UE ratios in small cell.

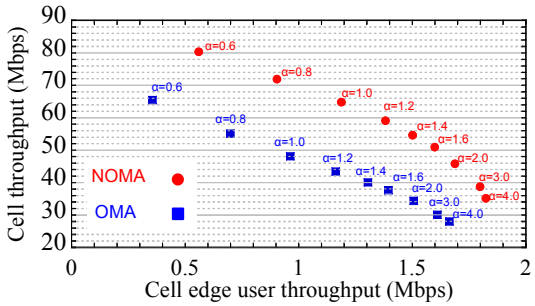

Fig. 5. Cell and cell-edge user throughput with different value of α.

V. Conclusion

In this paper, we evaluated the system–level performance of NOMA combined with OL SU-MIMO specified in LTE/LTE-A considering a various environment, including small cell. Based on computer simulations, we showed that the NOMA gain is still obtained even in a small cell. We also evaluated the performance gain of NOMA with various outdoor UE ratios. The simulation results show that NOMA provides a larger performance gain compared to that for OMA.

ACKNOWLEDGMENT

Part of this work has been performed in the framework of the FP7 project ICT-317669 METIS, which is partly funded by the European Union. The authors would like to acknowledge the contributions of their colleagues in METIS, although the views expressed are those of the authors and do not necessarily represent the project.

References

[1] 3GPP Workshop on Release 12 and Onwards: RWS-120002-RWS-120052, Ljubljana, Slovenia, June 2012.

[2] METIS ICT-317669-METIS/D6.1, "Simulation guidelines," Oct. 2013

[3] ITU-R Study Group 5 (SG5) Working Package 5D (WP5D).

[4] Report ITU-R M.2243 (IMT. UPDATE), WP5D, 2011.

[5] Y. Kishiyama, A. Benjebbour, H. Ishii, and T. Nakamura, "Evolution concept and candidate technologies for future steps of LTE-A," IEEE ICCS2012, Nov. 2012.

[6] A. Benjebbour, Y. Saito, Y. Kishiyama, A. Li, A. Harada, and T. Nakamura, "Concept and practical considerations of non-orthogonal multiple access (NOMA) for future radio access," IEEE ISPACS, Nov. 2013.

[7] Y. Saito, A. Benjebbour, Y. Kishiyama, and T. Nakamura, A. Li, and K. Higuchi, "Non-orthogonal multiple access (NOMA) for future radio access," *IEEE VTC spring 2013*, June 2013.

[8] K. Higuchi and Y. Kishiyama, "Non-orthogonal access with random beamforming and intra-beam SIC for cellular MIMO downlink," IEEE VTC2013-Fall, Sept. 2013.

[9] A. Benjebbour, A. Li, Y. Saito, Y. Kishiyama, A. Harada, and T. Nakamura, "System-level performance of downlink NOMA for future LTE enhancements," IEEE Globecom, Dec. 2013.

[10] Y. Saito, A. Benjebbour, Y. Kishiyama, and T. Nakamura, "System-level performance evaluation of downlink non-orthogonal multiple access (NOMA)," IEEE PIMRC 2013, Sept. 2013.

[11] A. Benjebbour, A. Li, Y. Kishiyama, H. Jiang, T. Nakamura, "System-Level Performance of Downlink NOMA Combined with SU-MIMO for Future LTE Enhancements", IEEE Globecom, Dec. 2014.

[12] 3GPP, TR 36.872 (V12.1.0), "Small cell enhancements for EUTRA and E-UTRAN - physical aspects," Dec. 2013.

[13] 3GPP TR 36.814 (V9.0.0), "Evolved Universal Terrestrial Radio Access (E-UTRA); Further advancements for E-UTRA Physical layer aspects," Mar. 2010.

[14] 3GPP RP-130590, Study on 3D-channel model for Elevation Beamforming and FD-MIMO studies for LTE. TSG RAN Meeting #60